Supporting information

In situ formation of Cu-Sn bimetallic catalyst for CO_2 electroreduction to formate with high efficiency

Experimental section:

Materials:

Copper nitrate trihydrate ($Cu(NO_3)_2 \cdot 3H_2O$) (99%), tin (Ⅱ) acetate ($Sn(acac)_2$), sodium 2,2-dimethyl-2-silapentane-5-sulfonate (DSS) (99%), Deuteroxide (D_2O) (99.9%) and Nafion 117 solution (5wt% in the mixture of lower aliphatic alcohols and water) were purchased from Aladdin. Ammonium hydroxide ($NH_3 \cdot H_2O$) (65%-68%), potassium hydroxide (KOH) (≥85%) and ethanol were purchased from Sinopharm Chemical Reagent Co., Ltd. Both CO_2 and N_2 had a purity of 99.999%, and were provided by Shanghai Chemistry Industrial Zone Pujiang Special Type Gas Co., Ltd. Deionized water was used in the experiments and all the chemicals were used without further purification.

Fabrication of Cu-Sn pre-catalyst:

In a typical process, 2 mmol $Cu(NO_3)_2 \cdot 3H_2O$ and 0.5 mmol $Sn(acac)_2$ were added to deionized water (30 mL). The mixture was stirred magnetically at room temperature until all materials were dissolved. To adjust the solution pH to 10, $NH_3 \cdot H_2O$ solution was dropped into the solution and kept stirring. After that, the mixture was transferred to a 100 mL Teflon-lined stainless-steel autoclave and heated to 150 ^oC in an oven for 22 hours. After cooling to room temperature, the obtained precipitate was collected by centrifugation with deionized water and ethanol for several times, and dried in a vacuum drying oven under 50 ^oC for 12 hours. Finally, the $CuSnO_x$ precursor was obtained. And then, the dried $CuSnO_x$ precursor was calcined in a muffle furnace under 500 ^oC for 3 hours with a heating rate of 2 $^oC\ min^{-1}$. The resulting Cu-Sn pre-catalyst powder was collected. In the process of synthesis, we also

explored the influence of Cu/Sn ratio on the catalytic activity. The total molar amount of metal cations was 2.5 mmol, and the Cu/Sn ratios of 9:1, 3:2, 2:3, 1:4 were synthesized. In order to explore the effect of Cu, the catalyst without Cu salt was used as comparison samples in the synthesis process and the other steps were the same with the preparation of Cu-Sn pre-catalyst.

Fabrication of 19.0%Cu-SnO_x bimetallic catalyst:

6 mg Cu-Sn pre-catalyst was added to the mixture of 600 μL acetone and 30 μL Nafion solution. The solution was sonicated for 30 minutes to form an uniform ink. Eventually, the ink was dropped onto the 2×2 cm^{-2} carbon paper, dried at room temperature, and in situ electrochemical reduction was conducted at -1.5 V vs RHE for 500s (which was named as 19.0%Cu-SnO_x catalyst, and the Cu/Sn ratios of 9:1, 3:2, 2:3 and 1:4, were named as 21.8%Cu-SnO_x, 14.5%Cu-SnO_x, 7.7%Cu-SnO_x and 3.2%Cu-SnO_x, respectively. The catalyst without Cu was named as SnO_x).

Morphological and structural characterization:

The structure and composition of the catalysts were determined by X-ray diffractometry (XRD, Rigaku Ultima Ⅵ X-ray diffractometer) with Cu Kα radiation (35 kV and 25 mA). Transmission electron microscope (TEM) and High-angle annular dark-field scanning transmission electron microscopy (HAADF-STEM) images were obtained using FEI Tecnai G2 F30 TEM microscope equipped with energy-dispersive X-ray spectroscopy (EDS) operated at 300 kV. The X-ray photoelectron spectroscopy (XPS) data were collected on AXIS Supra surfacce analysis instrument (X-ray monochromatic source, Al/Ag radiation, 1486.6/2981.2 eV) to analysis the elemental composition and valency. The peak value of C 1s at 284.6 eV was taken as reference to modify the charging effect. The concentration of the catalyst was determined by the inductively coupled plasma atomic emission spectroscopy (710-ES, Varian, ICP-AES).

Electrochemical measurements:

Electrochemical studies were carried out in an electrochemical flow cell consisting of a gas chamber, a cathode chamber and an anode chamber. The electrochemical measurements were conducted on the electrochemical workstation

(CHI 660E, Shanghai CH Instruments Co., China) equipped with a high current amplifier CHI 680c. An anion exchange membrane (Fumasep FAA-3-PK-130) was used to separate the cathode from the anode. Linear sweep voltammetry (LSV) scanning was performed in a three-electrode system, including the working electrode, nickel foam as counter electrode, and Ag/AgCl (saturated KCl solution) as reference electrode. For performance studies, 1.0 M KOH solution (pH=13.8) was used as the electrolyte, the rate of peristaltic pump was 40 mL min^{-1}, and the flow rate of CO_2 was controlled to 20 sccm by digital gas flow controller. The measured potential after iR compensation (4.0 ohms)=85% was calculated by $E_{(versus\ RHE)} = E_{(versus\ Ag/AgCl)} + 0.197\ V + 0.059 \times pH$.

Product analysis:

In order to test the CO_2 reduction performance, the catalysts were tested by potentiostatic electrolysis for 30 minutes. The gas products produced by CO_2RR were analyzed by gas chromatography (GC, Agilent-7890A) with TCD detector and the FE was calculated according to the formula: $FE=n\times F\times moles\ of\ product/Q_{total}\times 100\%$. (Q: charge (C); F: Faradaic constant (96485 C/mol); n: the number of electrons required to generate the product) The liquid products generated by 30 minutes potentiostatic reduction were analyzed by nuclear magnetic resonance (NMR) spectrometer (Bruker; Ascend 400-400 MHz), and the 400 µL electrolyte was mixed with 200 µL D_2O, 100 µL 200 mM phenol and 100 µL 6 mM sodium 2, 2-dimethyl-2-silapentane-5-sulfonate (DSS) solution for ^1H NMR analysis.[1] Phenol was used as internal standard for formaic acid, and DSS was used as internal standard for ethanol, acetic and isopropanol.

Double layer capacitance (C_{dl}) measurement:

An uniform catalyst ink was dropped onto a carbon paper as the working electrode. The electrochemical active surface area was directly proportional to the C_{dl} value and C_{dl} was determined by measuring the capacitive current associated with the double layer charge from the scan rate dependence of the cycle.[1] C_{dl} was estimated by plotting Δj (j_a-j_c) against the scan rate at 0.16 V vs RHE, where j_a and j_c were the anode and cathode current densities, respectively. CVs was conducted in the range of 0.11 V to 0.21 V vs RHE and scan rates ranged from 10 to 200 mV s^{-1}.

Electrochemical impedance spectroscopy (EIS) studies:

EIS measurements were performed in 1.0 M KOH aqueous at an open circuit potential (OCP) with an amplitudes of 5 mV over the frequency range 10^{-1}-10^{6} Hz.

Long-time durability test:

The long-time stability test was performed in 1.0 M KOH solution with the CO_2 flow rate of 20 sccm at the potential of -1.5 V vs RHE.

Table S1. The naming rules of catalysts.

Catalyst	**The mole ratio of Cu/Sn**	**High temperature Calcination (°C)**	**In situ activation (s)**
$CuSnO_x$	4:1	/	/
Cu-Sn pre-catalyst	4:1	500	/
21.8%Cu-SnO_x	9:1	500	500
19.0%Cu-SnO_x	4:1	500	500
14.5%Cu-SnO_x	3:2	500	500
7.7%Cu-SnO_x	2:3	500	500
3.2%Cu-SnO_x	1:4	500	500
SnO_x	0:2.5	500	500

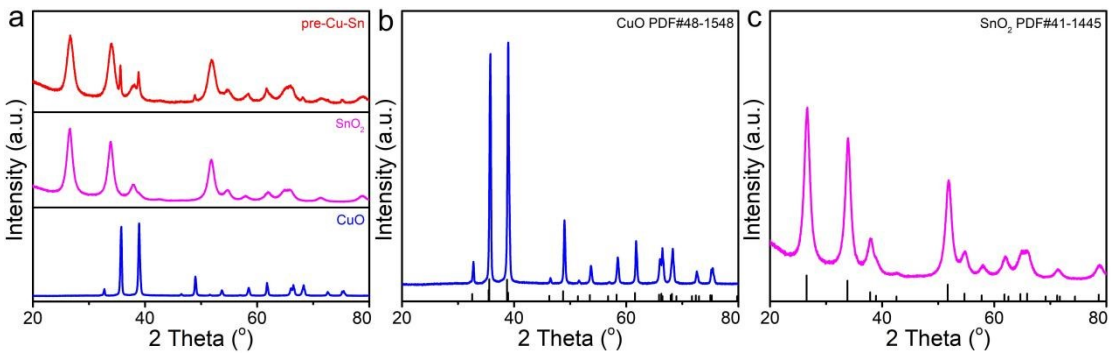

Figure S1. XRD patterns of (a) Cu-Sn pre-catalyst, (b) commercial CuO and (c) commercial SnO_2.

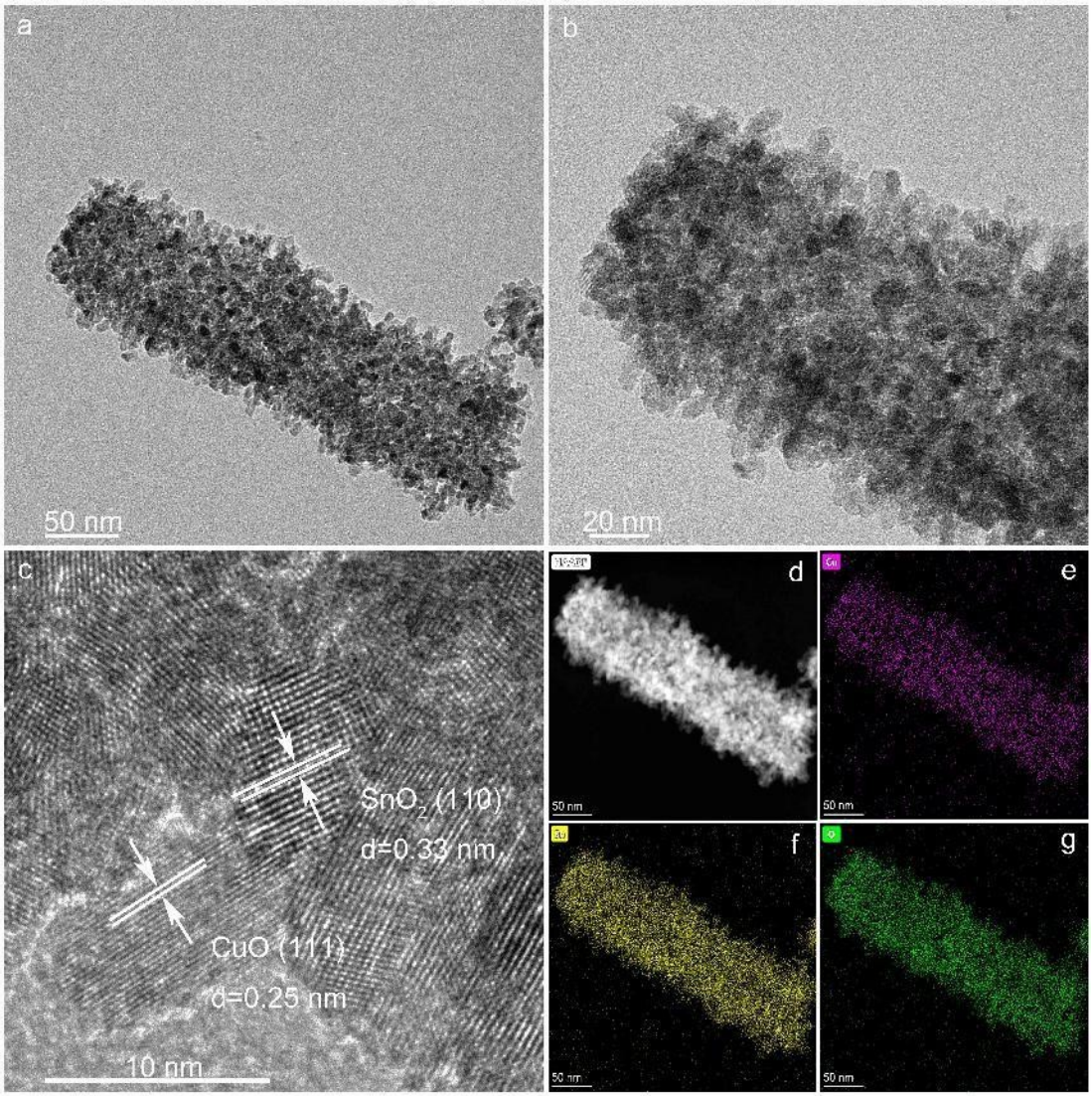

Figure S2. (a,b) TEM images and (c) magnified HRTEM spectra of Cu-Sn pre-catalyst. (d) HAADF-STEM image and the corresponding EDS elemental mapping images (e) Cu, (f) Sn and (g) O element of Cu-Sn pre-catalyst.

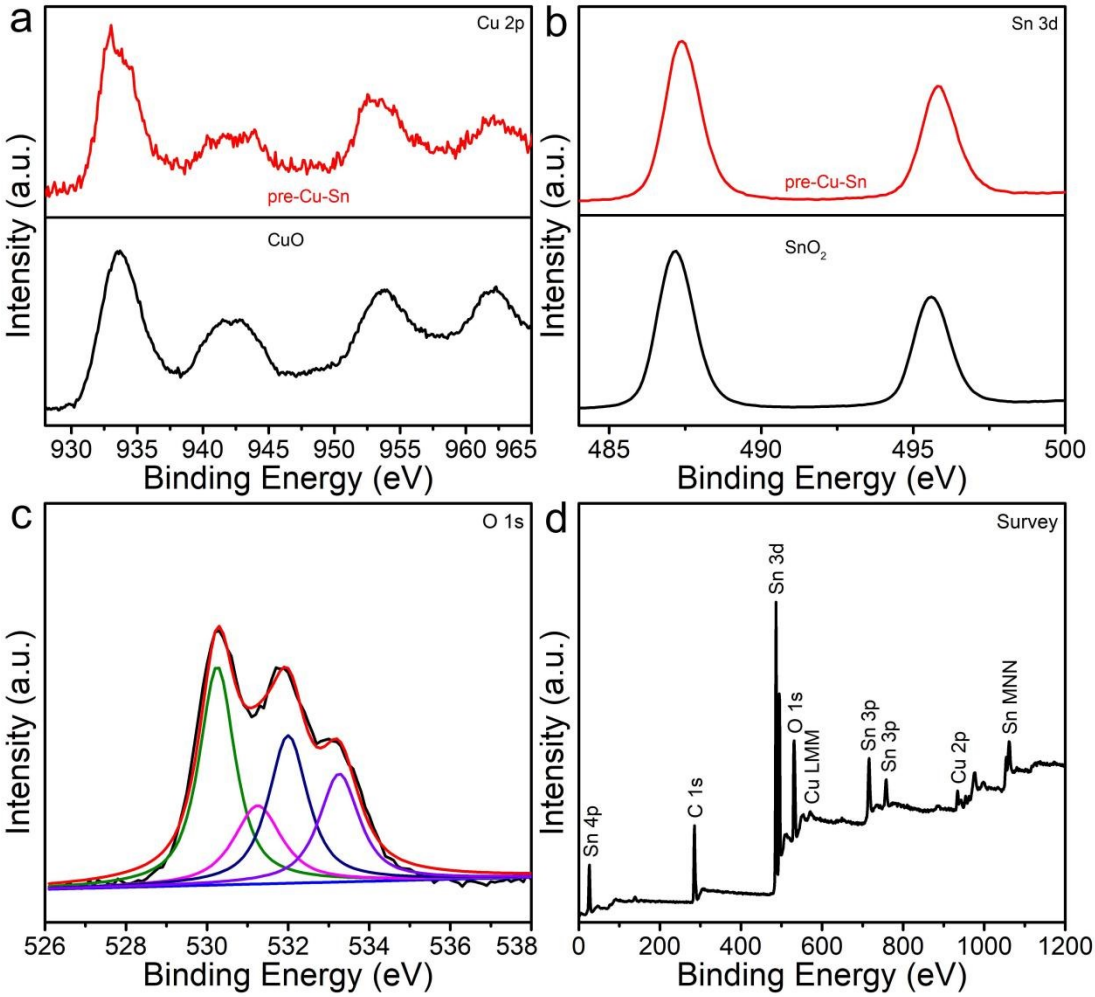

Figure S3. High-resolution XPS images of Cu-Sn pre-catalyst and commercial CuO and SnO_2. (a) Cu 2p and (b) Sn 3d, (c) O 1s and wide spectrum of Cu-Sn pre-catalyst.

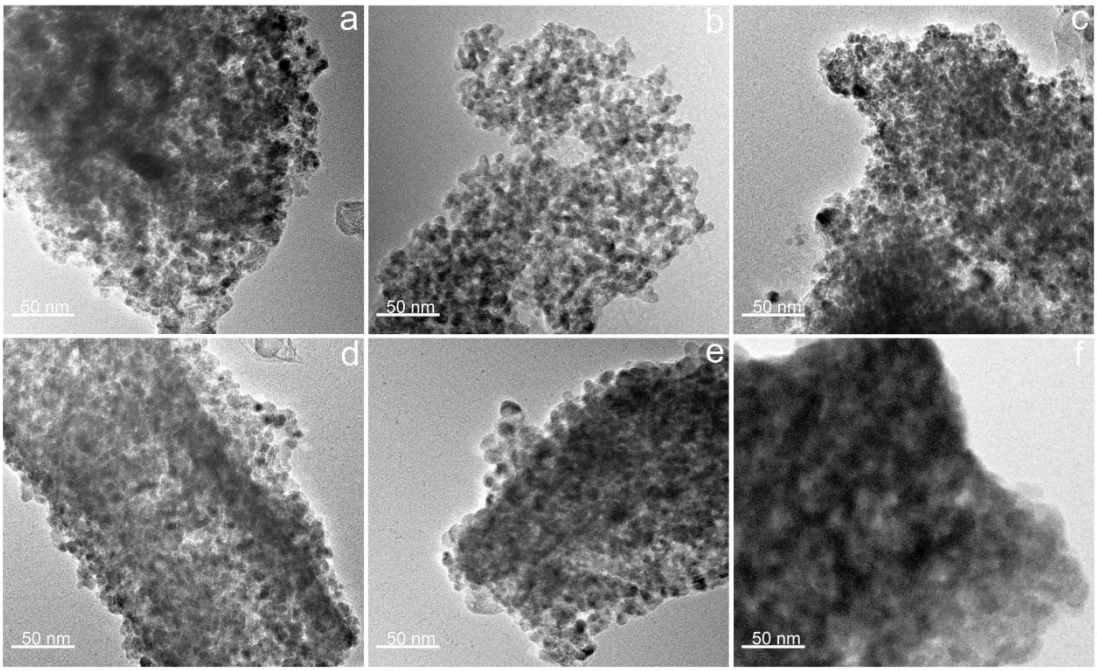

Figure S4. TEM images of different Cu/Sn ratio, (a) 21.8%Cu-SnO_x, (b) 19.0%Cu-SnO_x, (c) 14.5%Cu-SnO_x, (d) 7.7%Cu-SnO_x, (e) 3.2%Cu-SnO_x and (f) SnO_x.

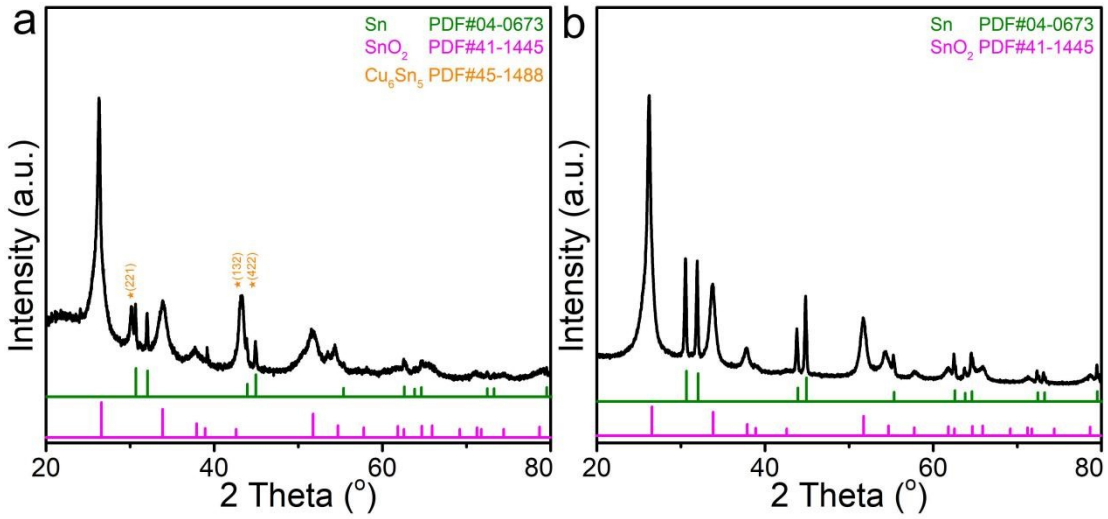

Figure S5. XRD images of (a) 19.0%Cu-SnO_x and (b) SnO_x after reconstruction.

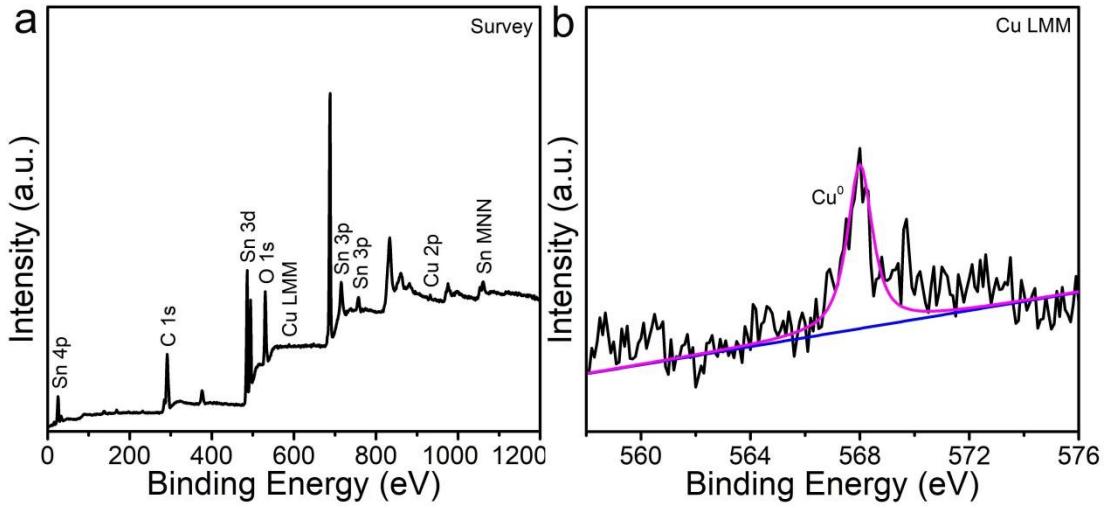

Figure S6. (a) XPS survey spectrum and (b) Cu LMM Auger spectra of 19.0%Cu-SnO_x.

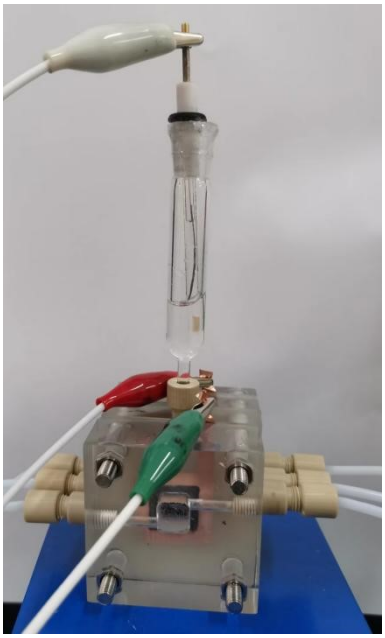

Figure S7. Schematic diagram of the flow cell configuration.

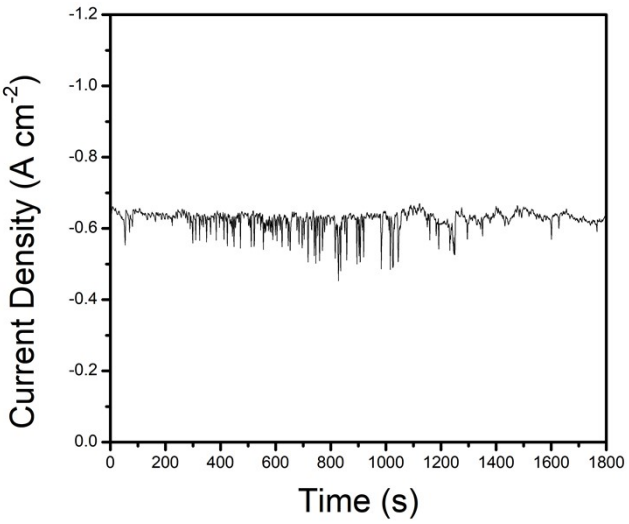

Figure S8. Diagram of 30 minutes I-t curve with iR=85%.

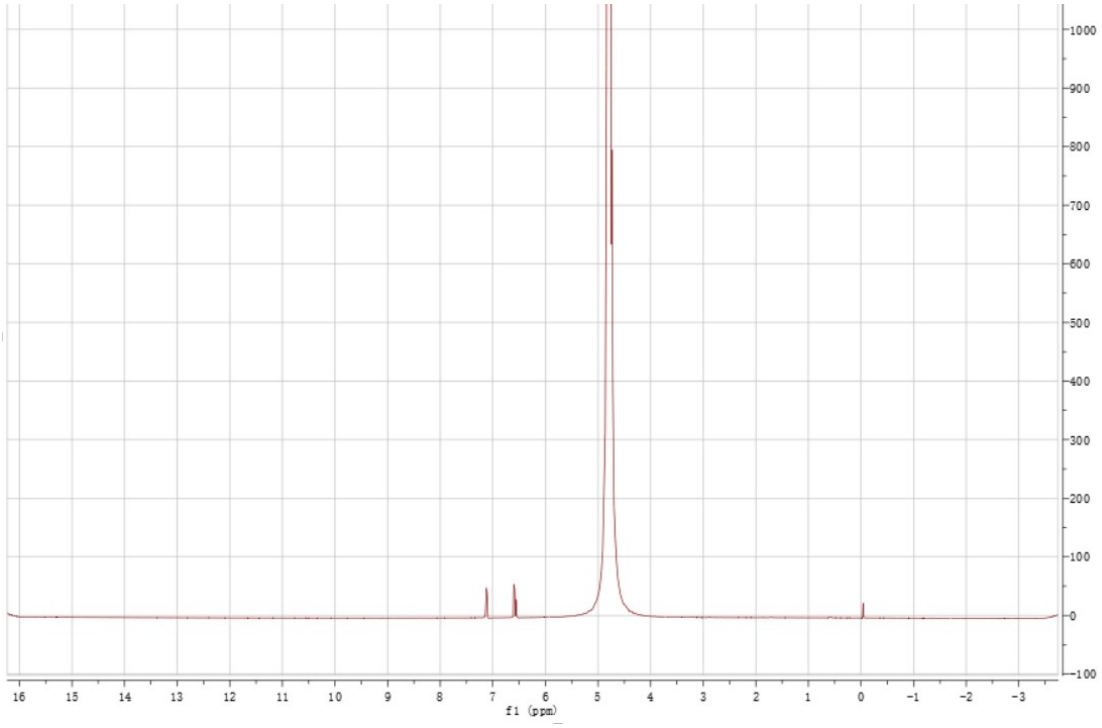

Figure S9. A typical ^{1}H NMR spectrum of liquid products in N_2 atmosphere over 19.0%Cu-SnO_x after 30 minutes I-t electrolysis.

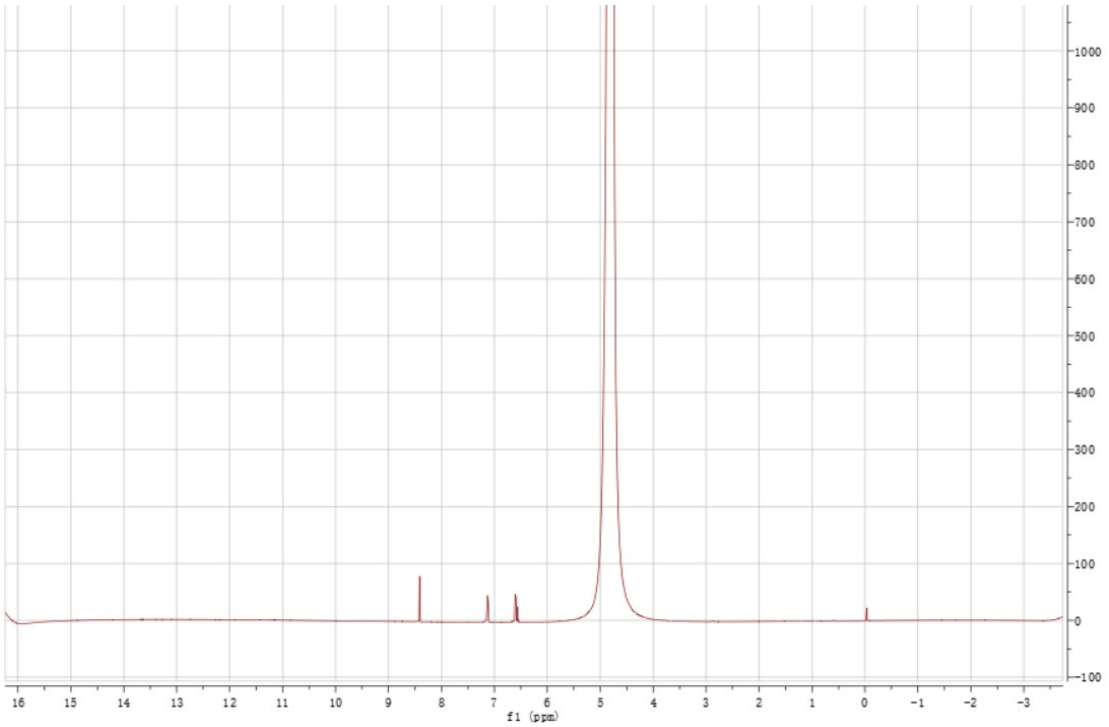

Figure S10. A typical ^{1}H NMR spectrum of liquid products in CO_2 atmosphere over 19.0%Cu-SnO_x after 30 minutes I-t electrolysis.

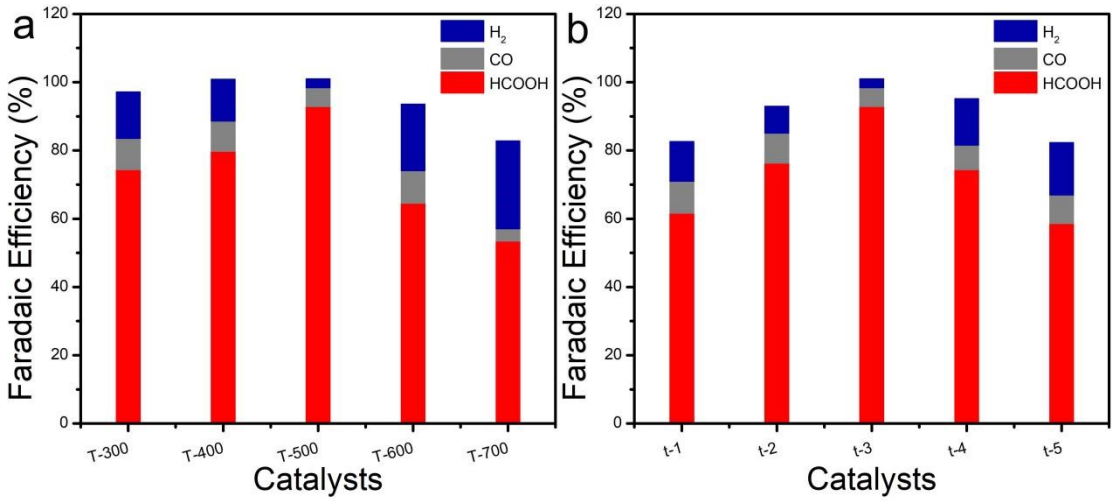

Figure S11. FEs of Cu-Sn bimetallic catalysts for CO_2RR with different (a) calcination temperature and (b) calcination time in 1.0 M KOH electrolyte.

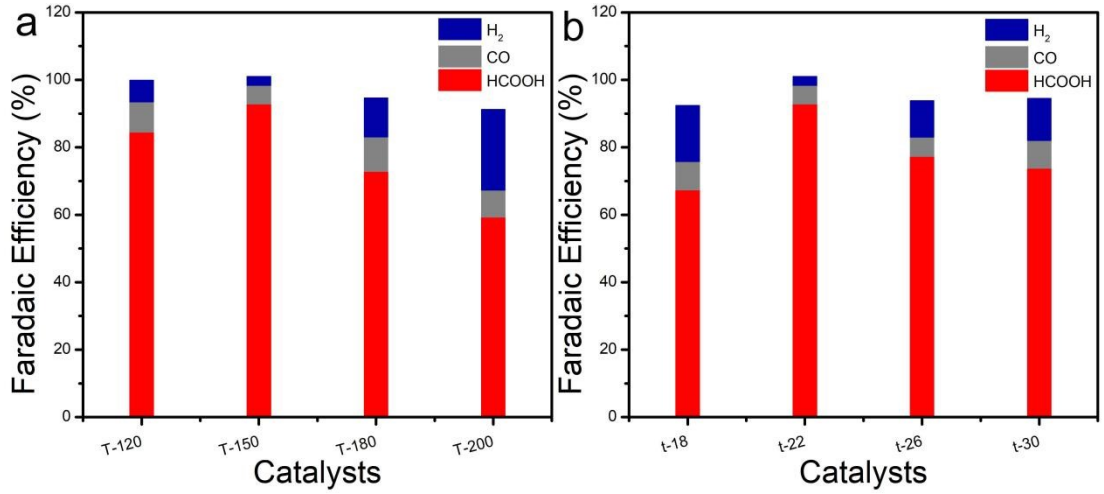

Figure S12. FEs of Cu-Sn bimetallic catalysts for CO_2RR with different (a) hydrothermal temperature and (b) hydrothermal time in 1.0 M KOH electrolyte.

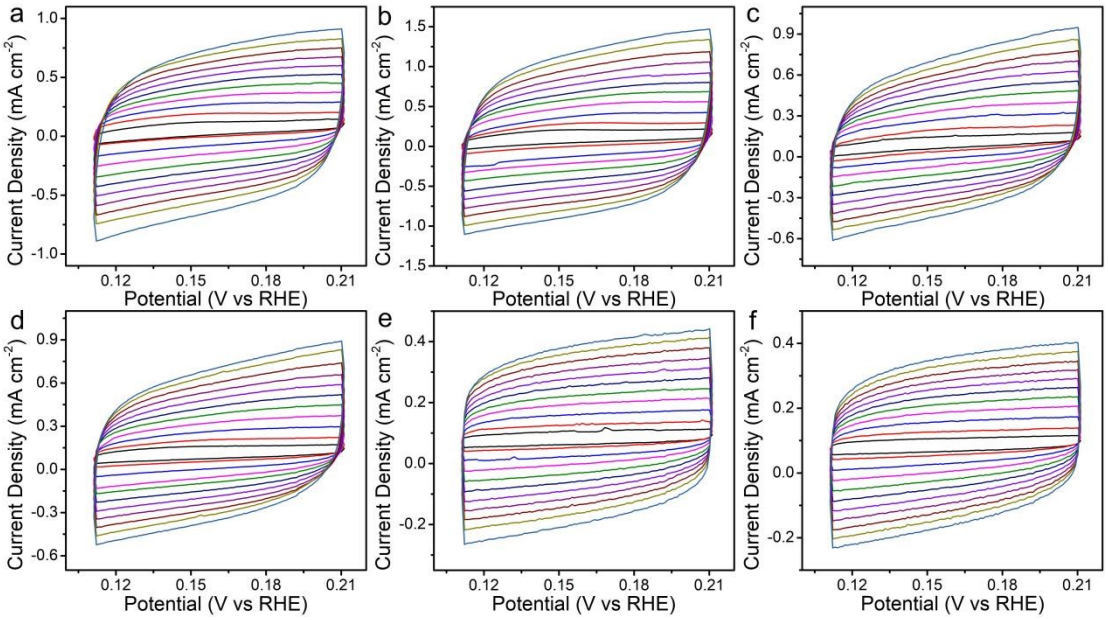

Figure S13. The cyclic voltammetry at various scan rates (10, 20, 40, 60, 80, 100, 120, 140, 160, 180 and 200 mV s^{-1}) over (a) 21.8%Cu-SnO_x, (b) 19.0%Cu-SnO_x, (c) 14.5%Cu-SnO_x, (d) 7.7%Cu-SnO_x, (e) 3.2%Cu-SnO_x and (f) SnO_x.

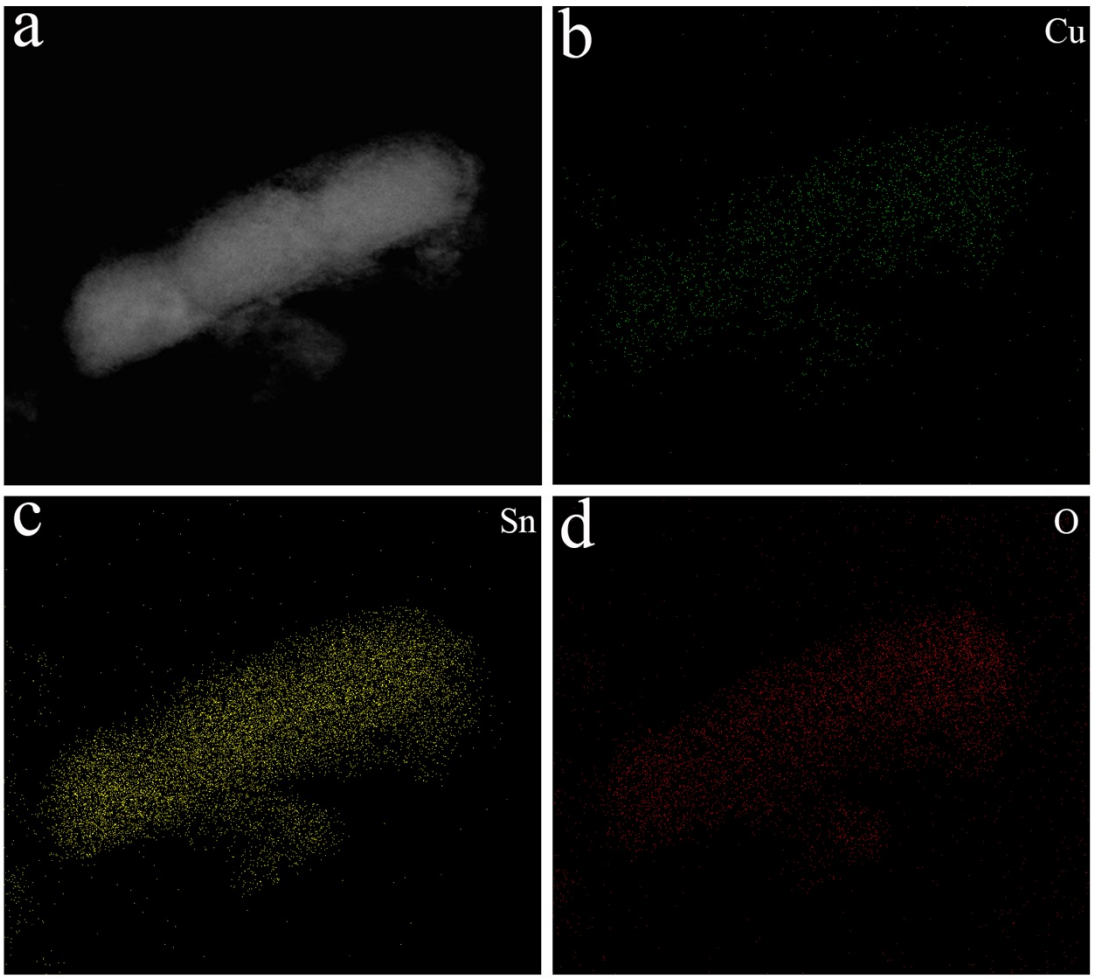

Figure S14. (a) HAADF-STEM image and (b-d) EDS spectra of 19.0%Cu-SnO_x after the long-term stability test.

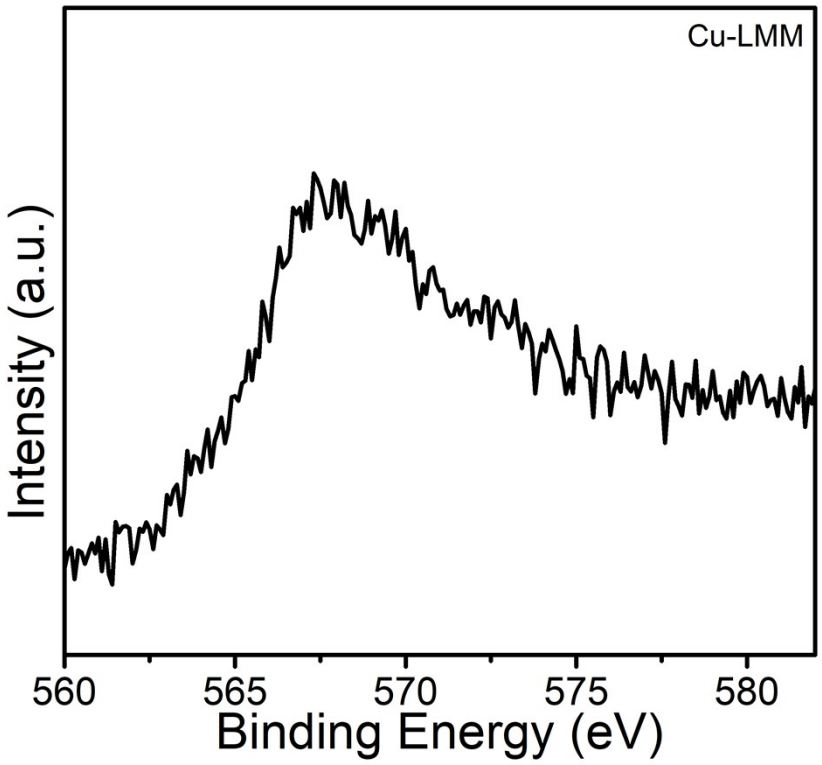

Figure S15. Cu LMM Auger spectra of 19.0%Cu-SnO_x after CO_2RR.

Table S2. Comparison of different Sn-based catalysts for HCOOH production by CO_2RR in flow cell.

Catalyst	**Electrolyte**	**Potential (V vs RHE)**	**Current Density (mA cm^{-2})**	**$FE_{(HCOOH)}$ (%)**	**Ref.**
19.0%Cu-SnO_x	1 M KOH	-1.5	632	92.9	This work
Cu_2SnS_3	0.5 M $KHCO_3$	-2.22	241	96.4	[2]
Cu_6Sn_5/Sn	0.5 M $NaHCO_3$	-1.0	118	86.69	[3]
SnO_2 nanosheets	1 M KOH	-1.13	471	94.2	[4]

Sn/SnO_2	1 M KOH	-1.3	116	79	[5]
Core-shell Sn-In alloy	1 M KOH	-0.98	236	94	[6]
$Sn_{2.7}Cu$ GDE	1 M KOH	-0.55	243.1	99	[7]
Cu_3Sn/Cu_6Sn_5	1 M KOH	-0.98	148	87	[8]
Hierarchical Sn_3O_4 nanosheets	1 M KOH	-1.02	421	91.1	[9]
SnO_2/CF	1 M KOH	-0.98	118	93	[10]
Sn	0.45 M $KHCO_3$+0.5 M KCl	-1.5	105	70.2	[11]
s-SnLi	1 M KOH	-1.2	1000	92	[12]
SnS nanosheets	1 M KOH	-1.3	120	88	[13]

Reference:

[1] X. Yan, C. Chen, Y. Wu, S. Liu, Y. Chen, R. Feng, J. Zhang and B. Han, *Chem. Sci.*, 2021, **12**, 6638.

[2] K. Li, J. Xu, T. Zheng, Y. Yuan, S. Liu, C. Shen, T. Jiang, J. Sun, Z. Liu, Y. Xu, M. Chuai, C. Xia and W. Chen, *ACS Catal.*, 2022, **12**, 9922-9932.

[3] Y. Wang, Y. Chen, Y. Zhao, J. Yu, Z. Liu, Y. Shi, H. Liu, X. Li and W. Zhou,

Appl. Catal. B-Environ., 2022, **307**, 120991.

[4] J. Li, J. Jiao, H. Zhang, P. Zhu, H. Ma, C. Chen, H. Xiao and Q. Lu, *ACS Sustainable Chem. Eng.,* 2020, **8**, 4975-4982.

[5] D. Kopljar, N. Wagner and E. Klemm, *Chem. Eng. Technol.*, 2016, **39**, 2042-2050.

[6] J. Wang, S. Ning, M. Luo, D. Xiang, W. Chen, X. Kang, Z. Jiang and S. Chen, *Appl. Catal. B-Environ.*, 2021, **288**, 119979.

[7] K. Ye, Z. Zhou, J. Shao, L. Lin, D. Gao, N. Ta, R. Si, G. Wang and X. Bao, *Angew. Chem. Int. Ed.*, 2020, **59**, 4814-4821.

[8] J. Wang, J. Zou, X. Hu, S. Ning, X. Wang, X. Kang and S. Chen, *J. Mater. Chem. A.*, 2019, **7**, 27514-27521.

[9] L. Liu, Y. Zhou, Y. Chang, J. Zhang, L. Jiang, W. Zhu and Y. Lin, *Nano Energy*, 2020, **77**, 105296.

[10] S. Ning, J. Wang, D. Xiang, S. Huang, W. Chen, S. Chen and X. Kang, *J. Catal.*, 2021, **399**, 67-74.

[11] A. D. Castillo, M. A.-Guerra, J. S.-Gullo´n, A. Sa´ez, V. Montiel and A. Irabien, *J. CO_2 Util.*, 2017, **18**, 222-228.

[12] S. Yan, C. Peng, C. Yang, Y. Chen, J. Zhang, A. Guan, X. Lv, H. Wang, Z. Wang, T.-K. Sham, Q. Han and G. Zheng, *Angew. Chem. Int. Ed.*, 2021, **133**, 25945-25949.

[13] J. Zou, C.-Y. Lee and G. G. Wallace, *Adv. Sci.*, 2021, **8**, 2004521.